Geomorphology 126 (2011) 186–200

Contents lists available at ScienceDirect

Geomorphology

journal homepage: www.elsevier.com/locate/geomorph

Airborne laser scanning of forested landslides characterization: Terrain model quality and visualization

K.A. Razak [a,b,*], M.W. Straatsma [a], C.J. van Westen [a], J.-P. Malet [c], S.M. de Jong [d]

[a] Faculty of Geo-Information Science and Earth Observation, University of Twente, P.O. Box 217, 7500 AE, Enschede, The Netherlands
[b] Universiti Teknologi Malaysia, UTM International Campus, Kuala Lumpur, Malaysia
[c] School and Observatory of Earth Sciences, Institut de Physique du Globe de Strasbourg, CNRS & University of Strasbourg, Strasbourg, France
[d] Utrecht University, Department of Physical Geography, Utrecht, The Netherlands

ARTICLE INFO

Article history:
Received 11 June 2010
Received in revised form 22 October 2010
Accepted 5 November 2010
Available online 8 December 2010

Keywords:
Airborne laser scanning
Forested landslides
Automatic bare-earth extraction
Landslide filter
Landslide visualization
Barcelonnette region

ABSTRACT

Mapping complex landslides under forested terrain requires an appropriate quality of digital terrain models (DTMs), which preserve small diagnostic features for landslide classification such as primary and secondary scarps, cracks, and displacement structures (flow-type and rigid-type). Optical satellite imagery, aerial photographs and synthetic aperture radar images are less effective to create reliable DTMs under tree coverage. Here, we utilized a very high density airborne laser scanning (ALS) data, with a point density of 140 points m^{-2} for generating a high quality DTM for mapping landslides in forested terrain in the Barcelonnette region, the Southern French Alps. We quantitatively evaluated the preservation of morphological features and qualitatively assessed the visualization of ALS-derived DTMs. We presented a filter parameterization method suitable for landslide mapping and compared it with two default filters from the hierarchical robust interpolation (HRI) and one default filter from the progressive TIN densification (PTD) method. The results indicate that the vertical accuracy of the DTM derived from the landslide filter is about 0.04 m less accurate than that from the PTD filter. However, the landslide filter yields a better quality of the image for the recognition of small diagnostic features as depicted by expert image interpreters. Several DTM visualization techniques were compared for visual interpretation. The openness map visualized in a stereoscopic model reveals more morphologically relevant features for landslide mapping than the other filter products. We also analyzed the minimal point density in ALS data for landslide mapping and found that a point density of more than 6 points m^{-2} is considered suitable for a detailed analysis of morphological features. This study illustrates the suitability of high density ALS data with an appropriate parameterization for the bare-earth extraction used for landslide identification and characterization in forested terrain.

1. Introduction

Landslides occur under a wide range of environmental conditions, including forested mountainous landscapes. Landslides often cause extensive damage and many casualties. Hence, it is important to identify landslides, define their characteristics, and assess the landslide susceptibility, hazard and risk. Landslide inventory maps are prepared by interpreting the geomorphic features of landslides on remote sensing imagery supported by field surveys. These maps yield insight into the locations of landslides, their typology and geometrical characteristics, the possible failure mechanisms, the state of activity and frequency of occurrences, the possible causal factors, and the historic damage (Van Westen et al., 2008). For sparsely or non-vegetated areas, various landslide mapping techniques are available, e.g. using single or multi-temporal aerial photographs (Brardinoni et al., 2003; Van Westen and Lulie Getahun, 2003; Prokesova et al., 2010), high spatial resolution satellite images (Nichol et al., 2006), or satellite-based synthetic aperture radar (Rott, 2009). In forested terrain, these techniques are less effective to identify landslides. Under closed forest canopies, visual interpretation of distinctive landslide morphological features is limited.

Over the last few years, airborne laser scanning (ALS) became available and is used to map landslide morphology and estimate landslide activity in areas that are partly or completely covered by dense vegetation (Sekiguchi and Sato, 2004; Van Den Eeckhaut et al., 2005, 2007; Glenn et al., 2006; Schulz, 2007). The ability of ALS to penetrate the forest canopy and its independence of solar incidence angle makes ALS superior to image-based photogrammetric techniques for acquiring a high resolution digital terrain model (DTM) in forested terrain (Kraus, 2007) and the high spatial resolution of ALS

* Corresponding author. Faculty of Geo-Information Science and Earth Observation, University of Twente, P.O. Box 217, 7500 AE, Enschede, The Netherlands. Tel.: +31 534874416; fax: +31 534874336.
E-mail address: razak@itc.nl (K.A. Razak).

0169-555X/$ – see front matter © 2010 Elsevier B.V. All rights reserved.
doi:10.1016/j.geomorph.2010.11.003

outperforms the use of synthetic aperture radar (SAR). The interpretability of landslides depends on the quality of the DTM. Reported vertical accuracies of vegetated and sloping terrains vary between 0.20 and 2.00 m (Huising and Gomes Pereira, 1998), 0.26 m for deciduous forests (Hodgson and Bresnahan, 2004), 0.57 m (Kraus and Pfeifer, 1998), 0.31 m for coniferous forest (Reutebuch et al., 2003) and 0.31 m for shrub and conifer trees (Wang and Glenn, 2009). So far no detailed assessment on DTMs has been carried out to reveal the suitability of ALS and derived DTMs to accurately map landslide morphological features.

ALS data are typically delivered as a very large dataset of points (clouds) with X, Y, Z coordinates (easting, northing and elevation). Various filter types are used to extract trees, houses or the bare-earth surface under trees from the raw dataset. Filtering of ground points from the ALS point cloud is an important step in the accurate geomorphologic mapping of landslides. Generally, ALS-derived DTMs have been used to characterize landslide morphology and activity (McKean and Roering, 2004; Glenn et al., 2006; Kasai et al., 2009). Several algorithms have been developed for DTM extraction from ALS point clouds (Sithole and Vosselman, 2004). In spite of the ability to automatically classify ground points and non-ground points, complex scenarios such as the preservation of discontinuities (e.g. steep slopes), vegetation on slopes, low vegetation and influence of outliers (e.g. multi-path errors or hit off objects) still require further improvement of the filtering algorithms (Sithole and Vosselman, 2004) and some manual editing is often carried out by the data provider. The selection of the appropriate filtering algorithm depends on the type and complexity of the landscape (Sithole and Vosselman, 2004; James et al., 2007). An optimal method for landslide inventory mapping is currently not known. Especially, the preservation of important landslide characteristics, such as scarps, cracks, rock blocks, deposition lobes, ponds, hummocky topography, and back-tilted slope surface, while removing vegetation is a challenging task. Therefore the first objective of this paper is to test the performance of two well known DTM filters, the hierarchical robust interpolation and progressive TIN densification, to quantify the error in the DTMs in rugged forested terrain focusing on geomorphological features of forested landslides. Herein, forested landslides refer to landslides that have occurred in the area that are partly or completely covered by vegetation. For this we acquired a very high resolution ALS data of more than 140 points m^{-2} to exclude point density as a limiting factor and to allow the determination of the appropriate point density for landslide mapping.

The second part of the paper evaluates various visualization methods of an ALS-derived DTM representing a large complex landslide. Different visualization techniques are discussed in the literature: monoscopic images (e.g. shaded relief, color composite and openness) and three-dimensional model (e.g. stereoscopic images and 3D point cloud visualization) approaches. We qualitatively assess the visual interpretability of a landslide DTM with respect to the characterization of landslide activity, and the mapping of scarps, rock blocks, displaced material and composition of the main slides and sub-slides using different visualization techniques. In this paper, a landslide DTM refers to the terrain model that shows the morphological features for landslide interpretability purposes. The evaluation was carried out by different image interpretation experts. Examples are taken from the Bois Noir landslide, located in the south French Alps, which is a complex landslide area involving several subset of landslide types (Flageollet et al., 1999; Thiery et al., 2007; Lopez Saez et al., submitted for publication).

2. Study area

The Bois Noir landslide (Fig. 1) is located on the south-facing slope of the Barcelonnette Basin in the South French Alps, 2.5 km to the south-east of Jausiers (Alpes-de-Haute-Provence, France). The area is characterized by irregular topography with slope gradients ranging between 10° and 35° (Thiery et al., 2007) and the site is covered by *Pinus Nigra* (black pine tree) which is the dominant species. Geology at the study area is characterized by a 15-m thick top layer of morainic colluvium, underlain by autochtonous Callovo-Oxfordian black marls as present in the northern part of the Bois Noir landslide (Maquaire et al., 2003). The southern part of Bois Noir is characterized by outcrops of limestone in the summit crest and is characterized by steep slopes of up to 70°, with extensive scree slopes.

The hummocky topography is inherited from the different phases of the Quaternary glaciation (Hippolyte and Dumont, 2002). The Bois Noir slope segment is characterized by a dry and mountainous Mediterranean climate with strong inter-annual rainfall variability (e.g. annual rainfall may vary between 400 and 1400 mm). These predisposing geomorphic and climatic factors explain the development of the slope by rotational or translational shallow landslides which usually affect the uppermost 2 to 6 m (Thiery et al., 2007).

Forest covers 92% of the total surface area and consists mainly of black pine with some deciduous trees (Thiery et al., 2004). All the landslides composing the landslide complex are typically shallow and occur at the interface between the bedrock and the surface deposits. In Thiery et al. (2007), this area has been identified as highly susceptible to landslides although most of the area is covered by vegetation. They created a landslide inventory map of 1:10,000 scale, based on aerial-photo interpretation, field surveys and historical records. Tilted and deformed trees, as well as recent scarps and open cracks, clearly indicate that the Bois Noir landslide has been subject to multiple reactivation in the recent past. We focussed on a small and most active part of the 24 ha of the Bois Noir slope segment (Fig. 1A) to limit data volumes and to optimize the scale of visualization.

3. Methods

3.1. Data collection

3.1.1. Field measurements

A field campaign was carried out in June 2009, during which terrain heights were measured using a Leica differential GPS system 1200. A total station was used to measure under dense canopies where the GPS signal was too weak for accurate positioning. We established two geodetic base stations to create a local geodetic network. Locations were selected based on open sky view for optimal reception of the GPS signals and to avoid the delayed signals affected by multi-path effects. A 24-hour static observation was carried out for each geodetic station. Horizontal and vertical accuracy of this equipment with static observation mode is about 3 and 10 mm at 0.5 ppm, respectively. Post-processing on the GPS data was done by taking the coordinate references from three available permanent GPS stations of RENAG (REseau NAtional GPS) located nearest to the study area. Position and baseline time series for the evaluation on the validity of the stations for reference are available online at http://webrenag.unice.fr. Horizontal and vertical precision of geodetic stations are on average 8 and 13 mm, respectively. Using these base stations, real-time kinematic GPS (RTK-GPS) was used to measure the terrain height. The GPS data were processed using strategy schemes implemented in Topcon Tools software version 7.2. The RAF98 geoid model was used to convert the ellipsoidal height into orthometric height. All the coordinates were projected into the local coordinate system, Lambert zone III using Lambert Conformal Conic with NTF (Nouvelle Triangulation de France) as datum.

In case it took too long or was not possible to get an accurate value using RTK-GPS, a total station was used. The position of the total station was determined using the two geodetic base points set up close to the forest boundary. From there, points under the dense tree canopy were measured and their accuracy is dependent on the geodetic station. A total of 332 points were collected over the study

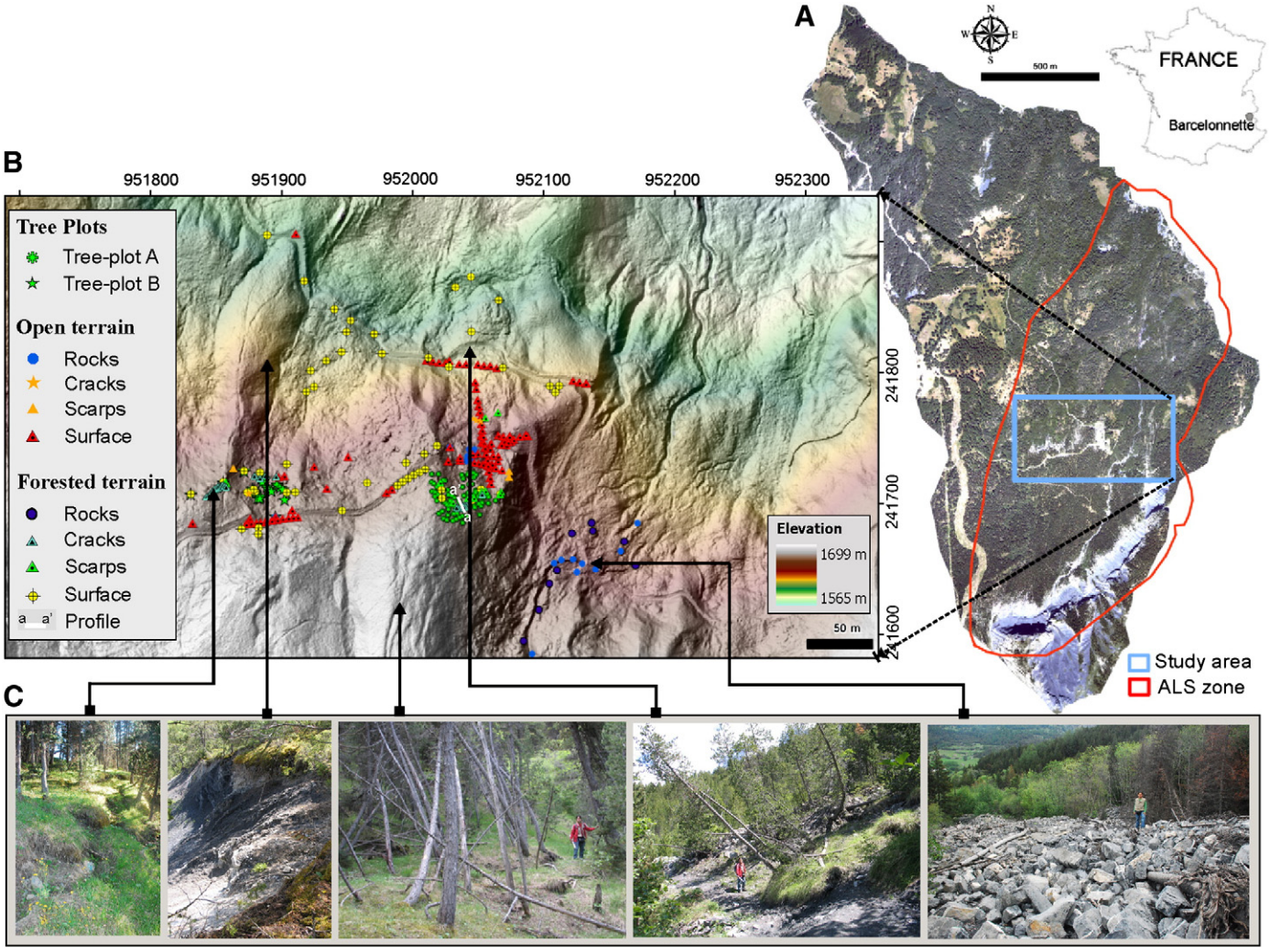

Fig. 1. Location of the study area at the Bois Noir landslide in the Barcelonnette Basin (South French Alps). A) Orthophoto of the study area and the ALS zone in 2009. B) Map showing validation points measured in different geomorphological features and trees over forested and open terrain. C) Photographs of representative landslides features in the study area.

area; they were distributed over geomorphological features such as scarps, cracks, blocks, depletion zones and accumulation zones (Fig. 1B). Two tree plots were measured, resulting in the terrain height at the location of 101 individual trees. Also a number of points were taken to represent the terrain height outside the geomorphological features.

3.1.2. ALS data acquisition

The ALS campaign was carried out under snow-free conditions in July 2009, using a helicopter flying about 300 m above the ground. An airborne hand-held laser scanning system provided by the Helimap Company was used. This system has been developed specifically for the mapping over mountainous forested areas (Vallet and Skaloud, 2004). A RIEGL VQ-480 laser scanner with a pulse repetition rate of up to 300 kHz was used to record full waveform laser data. Positioning was done using a Topcon Legacy GGD capable of tracking GPS and GLONASS positioning satellites. The orientation of the aircraft was determined using the iMAR FSAS inertial measurement unit (see Table 1 for details). In order to increase the point density seven flight lines were flown resulting in 50 million points. We used last pulse data that amounted to 35 million points with a mean point density of 140 points m^{-2}, which is still far above most commercial applications of ALS data.

3.2. Quantitative assessment of landslide DTM accuracy

In this study, we evaluated two common filters for bare-earth extraction (Sithole and Vosselman, 2004): hierarchical robust interpolation (HRI) and progressive TIN densification (PTD). Both filters execute automatically without manual editing and work on point clouds directly without gridding the data, so no information is lost by point to grid conversion. We tested the effect of different filter settings and assessed the result quantitatively against field reference data and qualitatively using different visualizations and knowledge from expert image interpreters.

Table 1
Metadata for the airborne laser scanning campaign.

Acquisition (month/year)	July 2009
Laser scanner	Riegl VQ480i
IMU system	iMAR FSAS — record 500 Hz
GPS system	Topcon legacy — record 5 Hz
Laser pulse repetition rate	300 kHz
Measurement rate	Up to 150 000 s^{-1}
Beam divergence	0.3 mrad
Laser beam footprint	75 mm at 250 m
Field of view	60°
Scanning method	Rotating multi-facet mirror

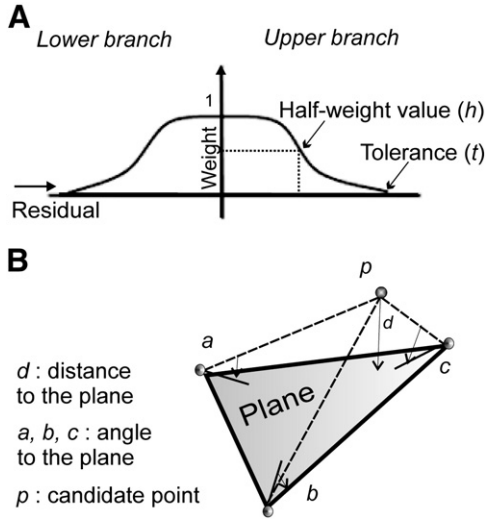

Fig. 2. Parameterization of hierarchical robust interpolation (HRI) and progressive TIN densification (PTD) methods. A) Weight function of the HRI method, showing the half-weight value (h) and tolerance (t) for residual calculation. B) Triangle of identified ground points indicate angles (a, b, and c) and distance to the plane (d) of the PTD method.

3.2.1. Parameterization of hierarchical robust interpolation

Robust interpolation was originally developed for ALS data in forested areas (Kraus and Pfeifer, 1998). A hierarchical approach was originally proposed by Pfeifer et al. (2001) and has similar structure to the image pyramids but the reduction function operates on the laser point data. The HRI method was embedded in SCOP++ software and has the capability to automatically extract points belonging to the ground surface and classify the non-ground points into several classes such as buildings, vegetation and low points.

At three different hierarchical levels that increase in resolution, four steps are carried out to extract ground points: thin out, filter, interpolate, and sort out/classify. In the thin out step, the original data are thinned out to a low density point cloud. A grid is overlaid over the point cloud, and for each cell, the lowest or most central point is chosen. In the filter step, a DTM is determined by applying the method of Kraus and Pfeifer (1998), which works by iteratively computing a local average. Weights are based on the residual value relative to the DTM in the previous iteration. The weight function gives a low weight to points with a large residual and high weight to points with a small residual. Fig. 2A shows a schematic diagram of a weight function which involves lower and upper branches for parameterization. The weight function has half of its maximum value at h and the weight function is cut off at tolerance, t. Next, a new DTM is defined by applying the linear prediction algorithm and in each step it is compared to the data of a higher resolution. In the sort out step, points within a certain vertical buffer are taken for the next iteration, and others are excluded. For the basic setting, we use 0.25 m as grid resolution and 0.15 m for mean accuracy of the point clouds. The value of the mean accuracy is considered by taking into account the mean errors produced by the differential GPS, inertial measurement unit and laser scanner system.

We proposed an iterative approach based on the HRI method, which we will refer to as the landslide filter. This filter is capable of dealing with the complexity of terrain, especially in a rugged forested area for landslide mapping. Besides that, we used two predefined parameterizations embedded in SCOP++, called as an HRI-default filter and a forest filter in this paper (Table 2). The forest filter is suggested for vegetated areas, whereas the HRI-default filter works best for areas with a mix of forest and open terrain. The landslide filter implements the robust interpolation in three schemes. Every scheme uses different parameters for the four steps as mentioned earlier and a number of points within the buffer zone as data input. Herein, a buffer zone refers to classified points (points on the ground and the points in between at the certain height of above and below ground surface). We assume that within the buffer zone, there are ALS points that belong to the landslide diagnostic features such as ALS points on the crown cracks and main scarps beneath the dense vegetation. In the first scheme, non-ground points are filtered out and only those points within 0.45 m buffer zone (taken from the ground surface to 0.225 m above and below it) are classified. This improved the estimate of a

Table 2
Parameterization of weight functions, thinning output and buffer zones for the landslide filter, forest filter and HRI-default filter.

Step/filter	Filter step — weight function				Thin out step	Classify step
	Upper branch		Lower branch			
	Half-weight value (m)	Tolerance (m)	Half-weight value (m)	Tolerance (m)	Cell size (m)	Buffer zone (m)
First hierarchy						
Landslide filter						
1st Scheme	0.80	2.40	–	3.60	3	0.45
2nd Scheme	0.56	1.68	–	2.52	3	0.20
3rd Scheme	0.40	1.20	–	1.80	3	0.10
Forest filter	0.80	2.40	–	3.60	6	0.45
HRI-default filter	0.80	2.40	–	3.60	3	0.45
Second hierarchy						
Landslide filter						
1st Scheme	0.30	0.90	1.20	1.20	2	0.45
2nd Scheme	0.21	0.63	0.84	0.84	2	0.20
3rd Scheme	0.15	0.45	0.60	0.60	2	0.10
Forest filter	0.30	0.90	1.20	1.20	3	0.45
HRI-default filter	0.30	0.90	1.20	1.20	2	0.45
Third hierarchy						
Landslide filter						
1st Scheme	0.15	0.30	0.23	0.45	0.25	0.45
2nd Scheme	0.11	0.30	0.16	0.45	0.25	0.20
3rd Scheme	0.08	0.30	0.11	0.45	0.25	0.10
Forest filter	0.15	0.30	0.23	0.45	0.25	0.45
HRI-default filter	0.15	0.30	0.23	0.45	0.25	0.45

DTM and therefore in the subsequent iterations more stringent limits are imposed on the filtering. For example, buffer zones of 0.2 and 0.1 m are used during the second and third scheme, respectively, and the values of h and t decrease further. By implementing this strategy, the residual to the true DTM is computed increasingly accurate, and less affected by vegetation or non-ground points for the second and third scheme. Hence, the bare-earth points are classified more accurately and the DTM accuracy is improved.

3.2.2. Parameterization of progressive TIN densification

The PTD method was developed by Axelsson (2000). It has been implemented in the Terrascan software and operates on point data. Starting with a sparse TIN, based on neighbourhood minima, the TIN is progressively densified to represent more local detail. In each iteration, points are added to the existing TIN if they are below predefined thresholds. The thresholds are determined on the basis of the angle points (a, b, and c) of the TIN facets and the distance (d) to the plane (Fig. 2B). The procedure to add candidate points (p) to the TIN is done continuously until all points exceed the thresholds. Parameterization of PTD consists of the selection of the maximum slope degree of the study area, the lowest points in a large grid, the maximum number of iterations for distance and angle to the plane, and threshold for the edge length. This predefined parameterization will be referred to as a PTD filter.

Due to the use of local minima, the PTD method is sensitive to below terrain blunders, which need to be removed before filtering. We removed all blunders points, defined as points with the next lowest points within the local window. Here, points 0.5 m lower than any neighbouring point within a 5 m radius are used. We set the maximum slope angle to 86°, the iteration angle to 10°, and the distance to the plane to 1.5 m. For the iteration angle, the edge length was set to less than 5 m in order to avoid adding unnecessary points and to reduce the use of memory and computation time. These choices are based on point density and terrain characteristics over the study area.

3.2.3. Quantitative error assessment

The vertical accuracy of the different DTMs is first determined by computing *RMSE* (root mean square error) between field points and a DTM as defined in the following equation:

$$RMSE = \sqrt{\frac{\sum_{i=1}^{n} (ZGPS_i - ZALS_i)^2}{n}} \quad (1)$$

where n is the number of field reference points, ZGPS are the terrain heights of points measured by GPS, ZALS are the predicted heights from the terrain model. *RMSE* was calculated for forested and open terrain and in both cases a further subdivision was made for scarps, cracks, rocks and ground surface. In addition, the DTM is evaluated under dense canopy at the locations of the tree plots. This procedure was applied to the DTMs derived from the four different filters.

The effect on the spatial representation of the four different DTM filters was assessed by computing the differences between the results from the landslide filter and the other filters. The last quality aspect evaluated is the density analysis of filtered points. The point density of the ground points is computed based on the average number of points within 1 m^2.

3.3. Qualitative assessment of DTM interpretability

The qualitative assessment of the ALS-derived DTMs produced by the different ALS filtering parameterization was carried out in two ways. Firstly, we assessed the interpretability of geomorphological features on a hybrid DTM, which consists of a regular grid, intermeshed with break lines, form lines, border lines and spot heights (SCOP++, 2008). Such DTMs have been used in many landscape studies, (e.g. Hollaus et al., 2006; Szekely et al., 2009). We assessed the interpretability of cracks, scarps, rock blocks, depletion zones and accumulation zones.

Secondly, we asked three expert interpreters to evaluate the interpretability of the different DTMs. The DTMs were provided to the expert image interpreters without informing them on the applied filtering methodology. The evaluation was done on the basis of a stereoscopic model and shaded relief images. The interpretability of different DTMs was rated based on the degree of morphological appearance and a landslide inventory map was created using DTM that was rated highest. The image interpretation was done using a screen visualization technique with 3D anaglyph glasses. A landslide map indicates the outlines of geomorphological units, roads, cracks, drainage network, and landslide activity.

3.3.1. Visualisation in 2D

The interpretability of the images depends on the DTM visualization techniques. Here we compare four different visualization techniques based on a gridded DTM with 0.25 m cell size.

- Shaded relief map (Horn, 1981). This technique applies an azimuth of 310° and an altitude of 40° for the sun's position.
- Color composite map (Smith and Clark, 2005). It is based on three shaded relief images with an azimuth in the West, North-West or North direction. Linear stretching was applied to the image.
- Openness map (Yokoyama et al., 2002). This technique generates an angular measure of surface form, unbiased from solar irradiation. It is computed from the zenith and nadir angles along eight DTM azimuths. Positive and negative openness indicates the convex and concave features of topography, respectively.
- Red relief image (Chiba et al., 2008). This technique produces a red image by adjusting the chrome value of red on the topographic slope and its brightness on the openness value. This image was prepared by Asia Air Survey Co. Ltd. using openness distance of 10 times of the grid resolution size of 0.25 m to optimize the visualization.

3.3.2. Visualization in 3D

Two types of 3D visualization were also produced and evaluated. The two 3D visualizations are one static and one dynamic presentation. Visualization in three dimensions was carried out using the following two techniques:

- Stereocopic model (Smith and Clark, 2005). A shaded relief and openness map and the DTM have been used to generate a stereoscopic view of the area.
- 3D point cloud visualization (Vosselman and Klein, 2010). This visualization technique offered a dynamic representation of the 3D point cloud as implemented in the Quick Terrain Modeler software version 7.1. The high density point clouds can visualize the representation of the relief and disrupted trees affected by landslides.

3.4. Analysis of ALS point density for landslide recognition

The ALS data enabled the acquisition of extremely dense point clouds over the landslide area. In this study, the point density of ALS data is 140 points m^{-2}. We have checked landslide interpretability of the ALS data at different point densities. The ground point dataset with an average of 53 points m^{-2} was thinned out progressively to derive eight data sets. The initial density was substantially reduced to end up with a density that is commonly used for generating ALS-derived DTMs. The eight datasets were categorized based on point grouping that have been used as thinning strategy. Horizontal distance of 0.25, 1, 3, 5, 7, 9, 11 and 13 m were used during the point grouping routine. At each thinning level, all the points within the given horizontal distance were grouped, and the thinning process stops after all the points were grouped. Next, the central points in

Table 3
Quantitative assessment of the vertical accuracy of morphological landslide features with different filter parameterization. Units are in meters.

	Cracks		Scarps		Rocks		Ground surface	
	Number of points	RMSE	Number of points	RMSE	Number of points	RMSE	Number of points	RMSE
Open terrain								
Landslide filter	5	0.33	5	0.40	18	0.33	94	0.34
Forest filter		0.33		0.39		0.39		0.35
HRI-default filter		0.33		0.87		0.41		0.35
PTD filter		0.29		0.36		0.32		0.31
Forested terrain								
Landslide filter	35	0.38	12	0.51	9	0.38	53	0.33
Forest filter		0.38		0.51		0.37		0.34
HRI-default filter		0.38		0.51		0.38		0.34
PTD filter		0.35		0.50		0.31		0.28

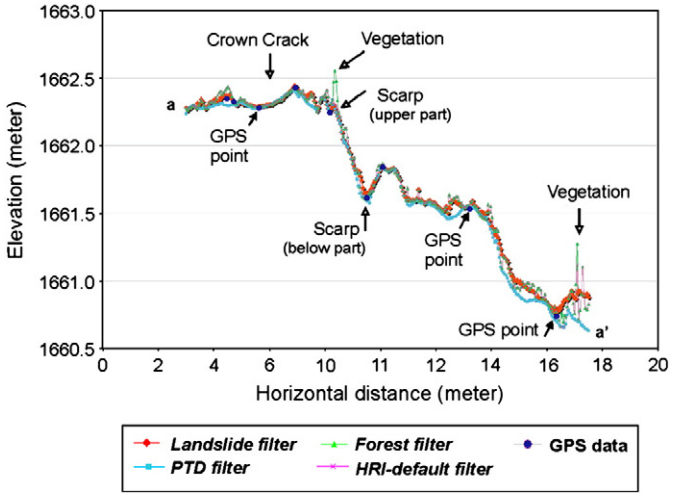

Fig. 3. Profile through the study area showing the results of the four filters together with the GPS measurements over a complex area. Location of the profile is shown in Fig. 1 (a–a′).

each group were also selected for the thinning dataset. This process was done using the algorithm implemented in Terrascan software. The eight datasets have different average point density in between 1.69 and 27.20 points m^{-2}.

Each thinned dataset was used to create a 1 m resolution DTM by using a natural neighbour interpolation technique. This interpolator is suitable to deal with rough terrain and is an essential step for the recognition of the morphological features (Pirotti and Tarolli, 2010). The original DTM and the eight thinned ALS-derived DTMs were given to expert image interpreters for suitability assessment. Diagnostic morphological features have been referred for this assessment in order to examine the suitability of ALS point density for landslide recognition. This assessment is informative for the users who want to order and use the ALS data for mapping landslides beneath vegetation.

4. Results

This study aims at evaluating the use of various ALS-derived DTMs for landslide mapping and identification of morphological features of landslides. The main results are presented and discussed in this section.

4.1. Quantitative assessment

The vertical accuracy of the four produced DTMs varies between 0.28 and 0.87 m compared to the field data and depends on the different morphological features and the applied filters (Table 3). For all morphological features the PTD filter outperforms the filters based on HRI with *RMSE* being lower than that for the best HRI parameterization by 0.02 to 0.04 m. The landslide filter shows the best results of the different HRI parameterizations. The errors for cracks and scarps are lower when no vegetation is present, but for rock blocks *RMSE* values are comparable between the open and forested terrain. The two tree sampling plots also show the PTD as the best filter and the landslide filter as the best HRI parameterization (Table 4).

Fig. 3 shows a line profile extracted from the DTMs produced by the four filters over an area covering crown cracks, main scarps and vegetated terrain. The location of the line profile (a–a′) is shown in Fig. 1. This area is delineated by the interpreters as a recent slide clearly showing an active scarp and crown cracks on the image. Nine GPS points were collected here for validation. The landslide filter works well for this area by preserving the crack on the upper scarp and the terrain morphology on the area below the scarp. The PTD filter shows a smoothening effect but still follows the roughness of the ground surface. In contrast, the forest and HRI-default filters still contain about ten points on the vegetation which are not properly filtered out (Fig. 3).

The original point density of last pulse data was 140 points m^{-2}. The point density of the ground points varies between 22 points m^{-2} and 76 points m^{-2} depending on the filters (Table 5). The point density of the filtered data using parameterization of the landslide filter is about 52 points m^{-2}, and 64% of the point cloud was filtered out during the automatic filtering process. For the second and third scheme of the landslide filter, the number of points was reduced to 46% and 36% of the original data. Point density of extracted ground points using the forest and HRI-default filters are about 76 points m^{-2} and 75 points m^{-2}, respectively. In contrast, point density analysis of the PTD method shows that the ALS points were reduced by 85% after the filtering process. The lesser number of ground points resulting

Table 4
Quantitative assessment of the vertical accuracy of vegetation features with different filter parameterization. Units are in meters.

	Tree — Plot A		Tree — Plot B	
	Number of points	RMSE (m)	Number of points	RMSE (m)
Landslide filter	22	0.34	79	0.36
Forest filter		0.40		0.37
HRI-default filter		0.41		0.37
PTD filter		0.32		0.33

Table 5
Point density of ALS ground points extracted using four different filters.

	ALS data input (million points)	Filtered ground points (Average points m^{-2})
Landslide filter		
First scheme	35.1	75
Second scheme	19.2	68
Third scheme	18.9	53
Forest filter	35.1	76
HRI-default filter	35.1	75
PTD filter	35.1	22

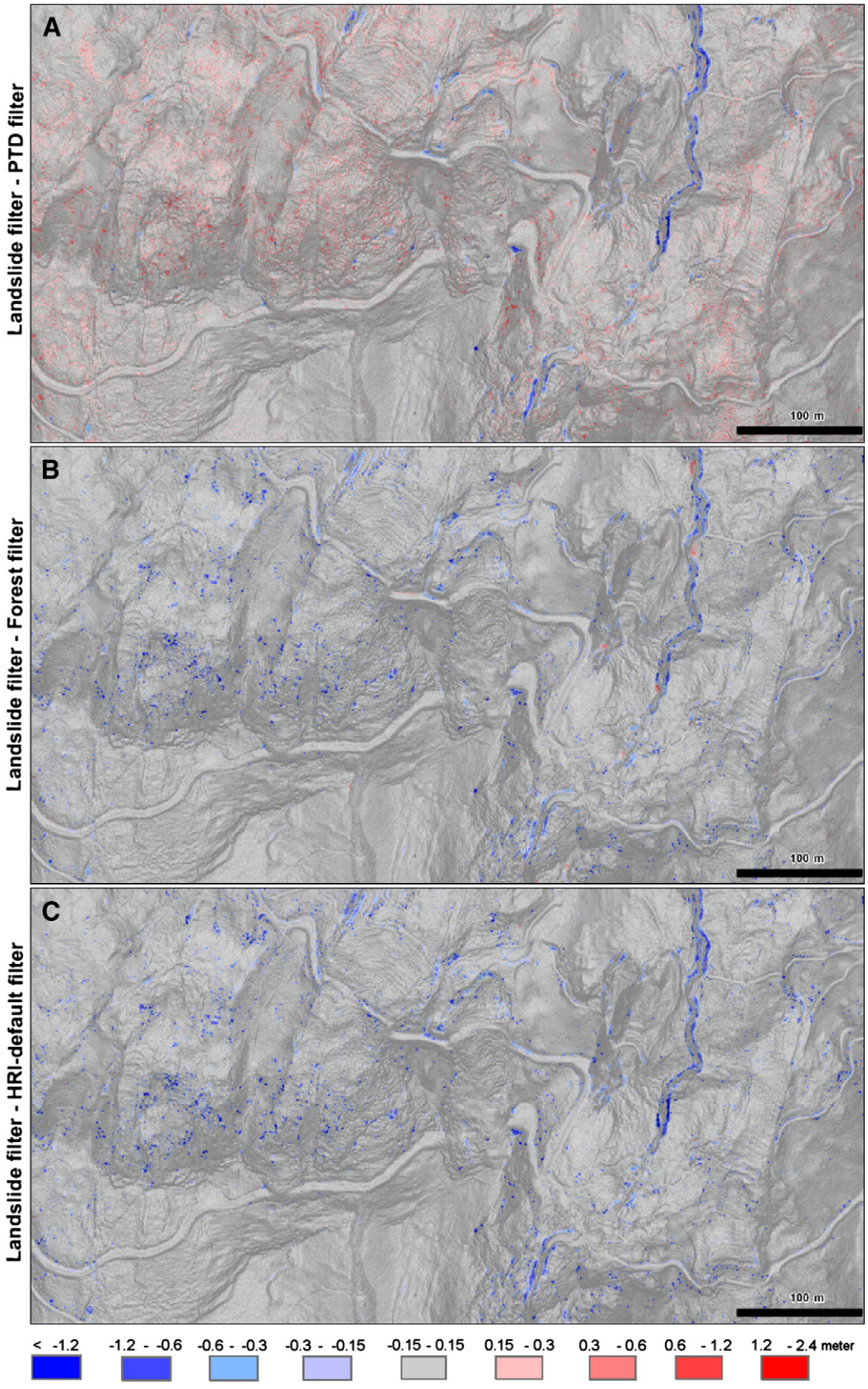

Fig. 4. Height differences between terrain models generated from the landslide filter- and A) PTD filter, B) forest filter and C) HRI-default filter. Positive values indicate that the DTM from the landslide filter is higher than the one from the other filter.

from the PTD filter leads to insufficient points to represent the diagnostic landslide morphological features and thus, a less accurate landslide DTM for forested landslide recognition.

The differences between the DTMs generated by the landslide filter and the other filters were computed to evaluate the spatial effect of the different filters (Fig. 4). The major height difference between the landslide and PTD filters mostly takes place over the zone of depletion as depicted in the two subset area in Fig. 4A. It shows that the landslide filter preserves small scale morphological features on such areas better than the PTD filter. In Fig. 4B and C, height differences between the landslide filter and both default filters indicate that most of the active landslide areas show altitude differences up to 0.15 m, whereas, over forested area, the height difference is up to 0.30 m. Significant height differences also show up in areas with a higher slope and along the stream incisions. Consequently, the Fig. 4B and C show more points that are not completely filtered out over open terrain and forested area.

4.2. Qualitative assessment of ALS-derived DTMs

The qualitative analysis on the generated DTMs by different filtering parameter settings was carried out based on shaded relief images of the hybrid DTM model as shown in Fig. 5. The reference image is the terrain model generated by the landslide filter. Fig. 5A presents an area with a number of shallow cracks in the terrain. Each of the filters is capable of identifying the cracks although the HRI-default filter and the forest filter still show some vegetation that was not properly filtered out. Fig. 5B indicates that the landslide and PTD

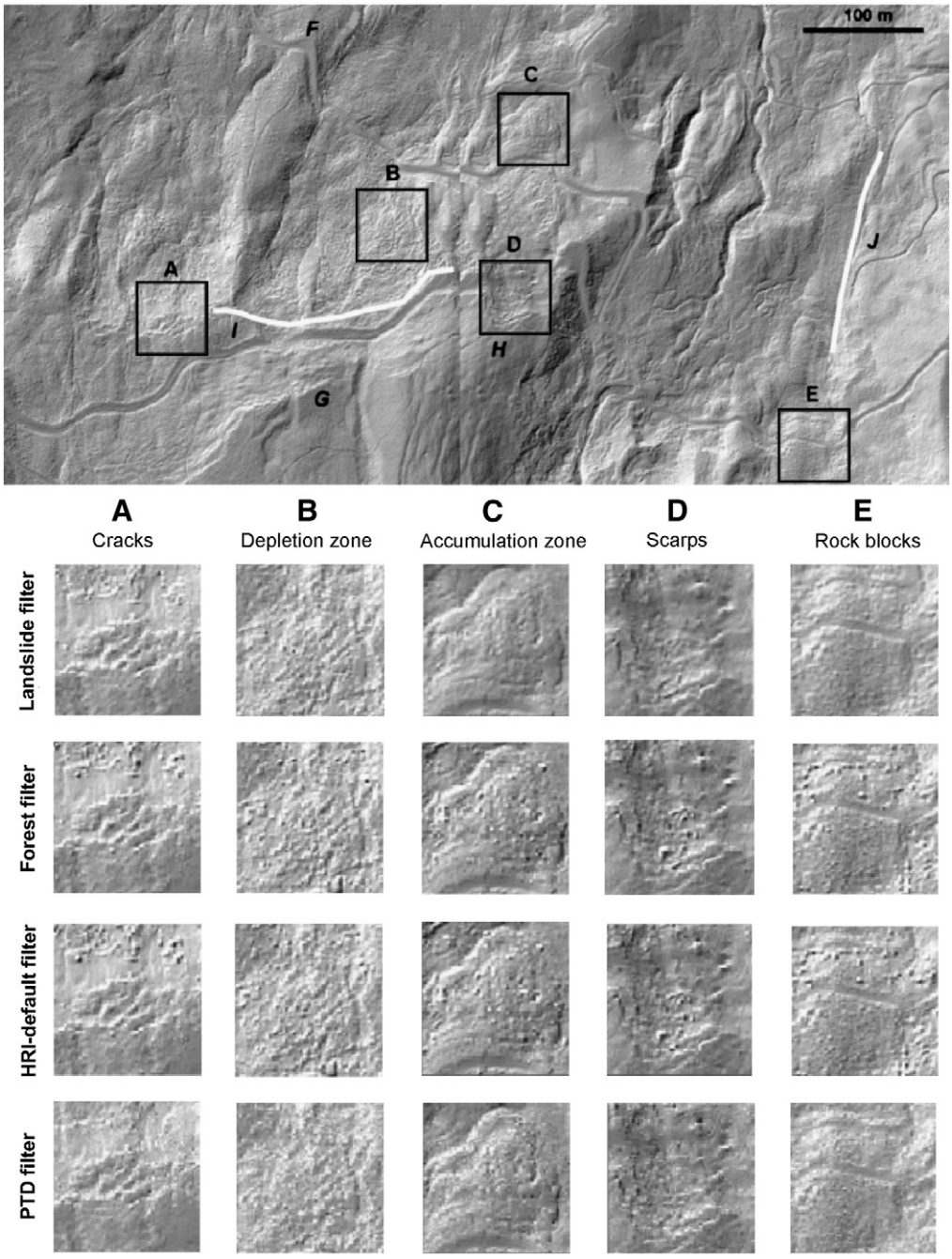

Fig. 5. Examples of the representation of the shaded relief images from hybrid DTM models from the four filters for different landslide features. See text for explanation.

filters are slightly better in eliminating trees compared to the other two filters. The accumulation zones in the complex landslide can be recognized on each of the filter products. The displaced material and the disrupted road are seen on the subset images (Fig. 5C). In Fig. 5D, the landslide filter shows slightly better results than the other filters for an escarpment area. However, as can be seen in Fig. 5E, the trade-off for the good performance is that both the landslide and PTD filters are worse for detecting isolated rock blocks in the area. The PTD filter also shows a smoothening effect due to insufficient ground points over the tested area.

4.3. Expert interpretation of DTMs

The three experts on image interpretation that evaluated the results from the various filters agree that the ALS-derived image generated using the landslide filter was the best for landslide interpretation. The PTD-derived DTM shows less information over the deposition and accumulation zones, whereas, the forest and HRI-default filters do not completely filter out the trees.

Fig. 6 shows the diagnostic features of landslides on openness images derived from DTM constructed with the landslide filter. The presence of clear cracks (A), semicircular niches followed by concave slopes (B), flow lobes with concentric patterns (C), hummocky terrain (D) and several secondary geomorphological features can be clearly observed. The recognition of small cracks might be the best feature that can be interpreted from these images, which provides additional information as compared to the interpretation of optical images such as aerial photos or satellite images. The forest cover in this area hides most of these landslide features, except for the few active zones, and makes the interpretation of the landslides very difficult from optical images.

Mapping landslide types is also possible, since the diagnostic features are interpretable on the images with a spatial resolution of

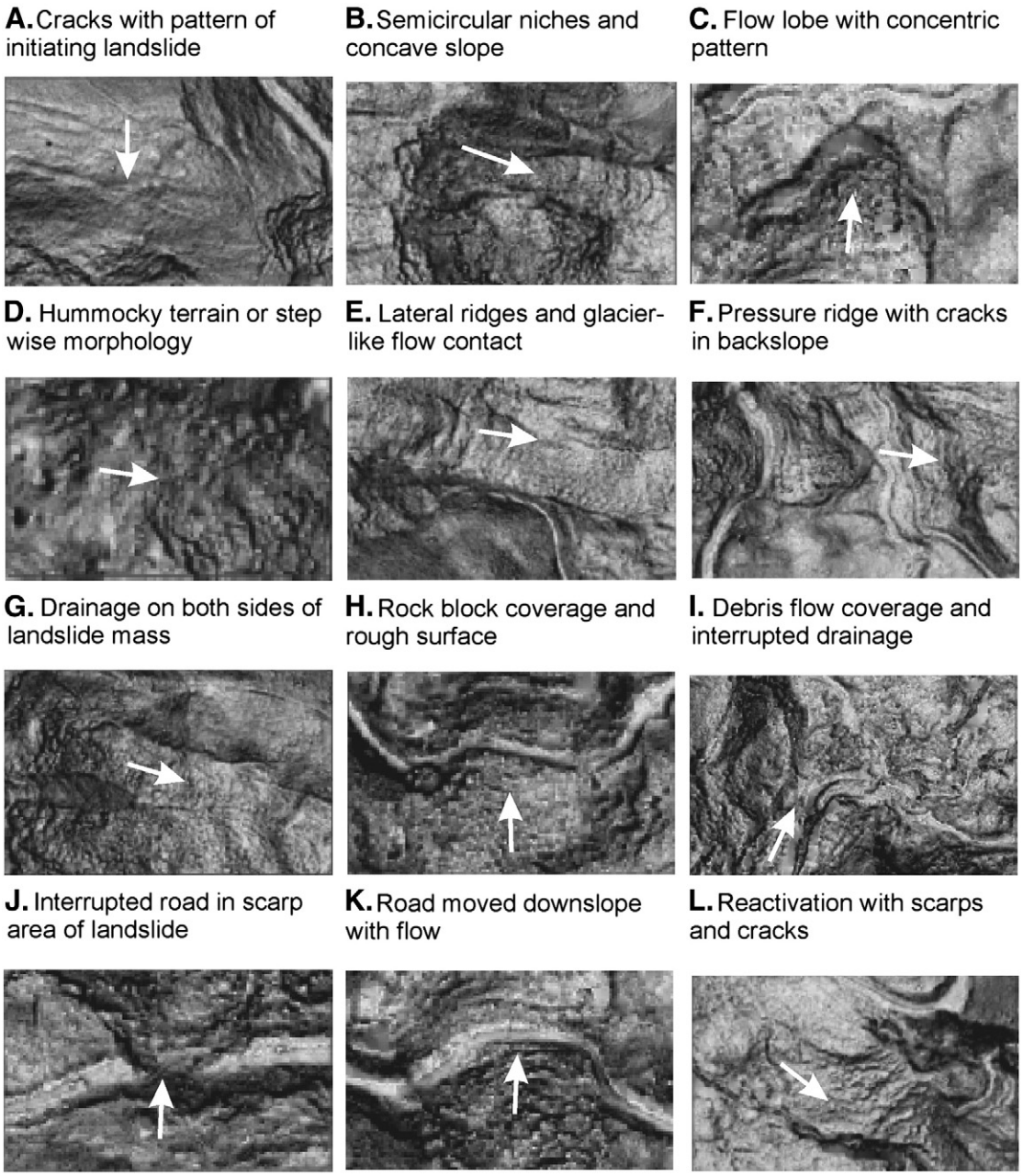

Fig. 6. Diagnostic features for the interpretation of landslide type and activity using the openness image from ALS, as indicated by expert image interpreters. The white arrows indicate the direction of landslide movement.

0.25 m. Most of the landslides in the study area have a source area where cracks are developed with a radial pattern, followed by a rotational landslide scarp (Fig. 6B). Most of the landslides are flow-type slides, and the landslide rigid body turn progressively into a flow-type body characterized by lobes with concentric ridges and cracks (Fig. 6C). There are also indications of mass flows that reach less steep slopes and that cannot extend laterally, producing pressure ridges with higher elevations, and large cracks in the upslope part (Fig. 6F). Another clear feature indicating flow-type behaviour is found in the East of the study area, where the mass flow of a larger landslide that enters the area from the South is separated from the surrounding terrain with lateral ridges (Fig. 6E).

The classification of landslide activity is more difficult based on only monoscopic images of filtered ALS data. As the information on vegetation characteristics is removed, it is not possible to use the presence of disrupted vegetation as a possible diagnostic feature. It is advisable to combine the interpretation of ALS-derived images with aerial photographs to get the best results. One of the best features that can be used in this case was the state of the roads and tracks that pass through the area. Interrupted roads (Fig. 6J) can be found in several places indicating recent landslide activity that took out the road surface. Also the downslope movement of the road surface on a landslide (Fig. 6K) is a clear diagnostic feature. The freshness of landslide features can only be used to classify the landslide in different classes of activity and relative age, although in this area most of the features appear rather fresh indicating that the entire area has been subjected to landslide activity very recently (Lopez Saez et al., submitted for publication). With the help of the openness map it is possible to map out the various phases of landslide activity, as many features are intersected by scarps and flow patterns of more recent events. This allows the reconstruction of the various phases of landslide activity. The interpretation indicates that the landslide history has been very complex with many phases of mass flows that overlap or are reactivated (Fig. 6L).

There are a number of aspects that are still unclear in the image and need further evaluation. This is partly because the image is covering part of a larger landslide complex (Bois Noir) and that there are features of older landslide phases which can only be properly interpreted when a larger area is evaluated. A complete geomorphological interpretation of the sample area is presented in Fig. 7. One of the questions that remained after interpreting the images is whether a number of ridge features (*F* and *G* in Fig. 5) have a structural geological control (for instance showing the bedding or the main local discontinuity of the underlying rocks) or are related to older landslide features. Given the importance of landslides in the area and the relatively large depth of the landslide features, it is more likely that these ridges are related to larger scale instability that can only be interpreted well when looking at the image of the entire Bois Noir landslide slope segment. Also the relationship between the most recent landslide activity and larger scale instability features (*H* in Fig. 5) should be further investigated. It appears that the recent landslide near *H* is actually occurring in a landslide block that is

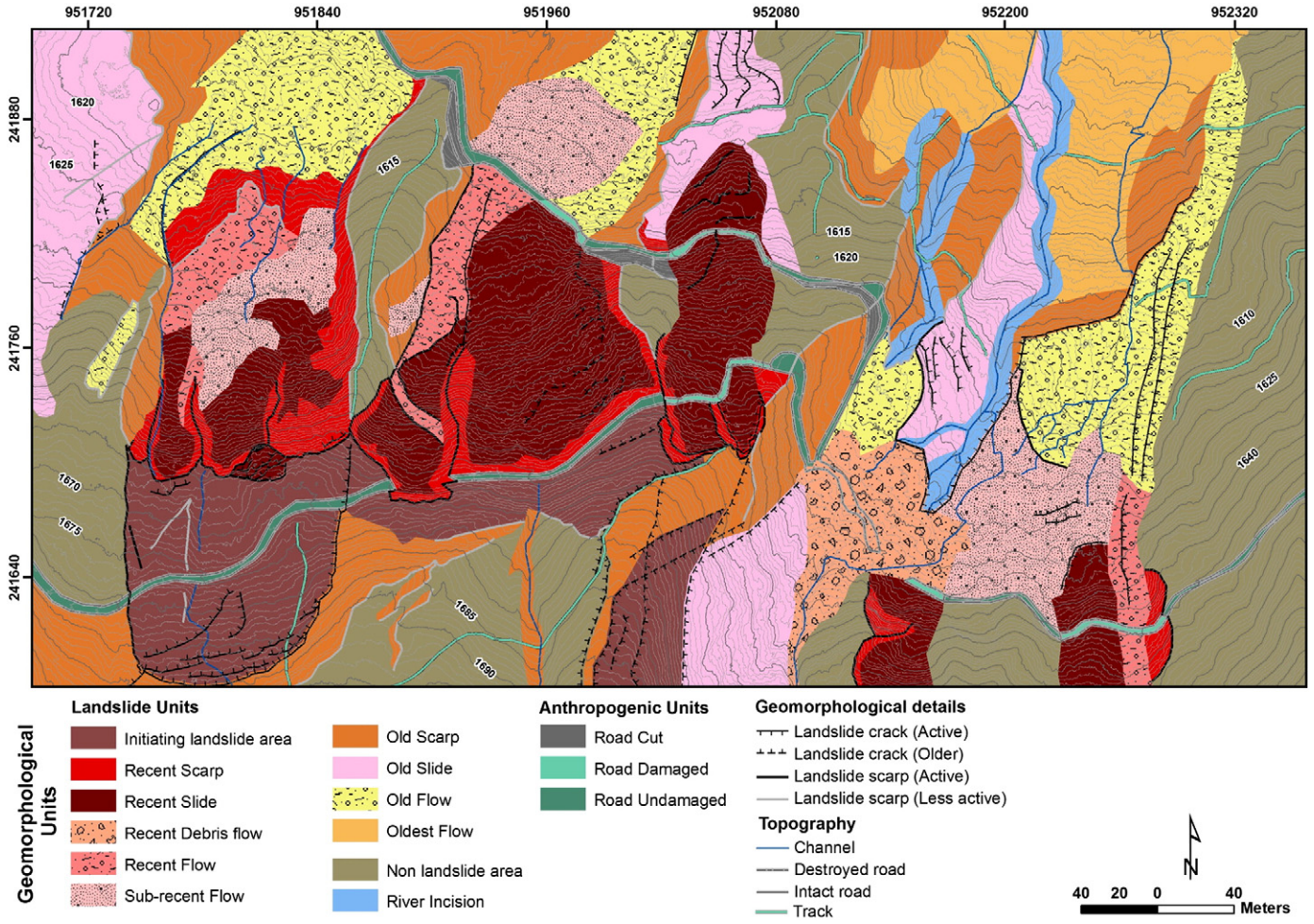

Fig. 7. Geomorphological map with classification of landslides created by the expert image interpreters.

located directly upslope. The line of reactivation (*I* in Fig. 5) seems to be related to an older landslide mass coming from upslope, as well as the large glacier-like flow structure (*J* in Fig. 5). The area between *H* and *J* is considered as a large flow accumulation which has had several stages of reactivation.

The landslide inventory map (Fig. 7) is prepared by the expert interpreters. The map combines the relative age of the landslides with morphological features and the landslide types. The areas indicated as "non-landslide area" are the side slopes and ridges between the landslide masses. They could be part of a larger, and older, landslide complex, but this can only be interpreted from images of a larger area. The source area is characterized by a large density of small cracks. They appear upslope of the actual active landslide area. The active landslides appear in a linear zone, probably related to a step in a larger landslide complex, and seriously affect the forest road in four places, two in the scarp area and two in the accumulation area of the active landslides. The eastern part of the area consists of a mass large flow, and which is reactivated in several places.

4.4. Visualization methods

The different 2D visualizations of the study area are presented in Fig. 8. The shaded relief image is less effective in highlighting micro-morphological features and it is difficult to identify features that occur parallel to the source areas of the landslides due to the illumination direction. This image requires a directional light source. The colour composite technique significantly improves the quality of the image in terms of visibility of some morphological features such as flow pattern and hummocky topography. The openness image is recognized by the image interpreters to be more appropriate for landslide visualization. Based on the qualitative assessment carried out on monoscopic images by expert image interpreters, many more macro- and micro-morphological features can be found on the openness map compared to the shaded relief map. The red relief image has similar interpretability as the openness map, but the image interpreters found the overall red colour to be disturbing in the image interpretation process. Small details are visible in the scarps and accumulation zone.

The 3D visualizations of the non-filtered and filtered datasets are shown in Figs. 9 and 10. The stereoscopic model presented as an anaglyph in Fig. 9A shows that most of the landslide morphology are hidden beneath dense vegetation, whereas geomorphological features under forest are clearly seen in Fig. 9B. Fig. 10A presents 34.2 million points cloud over the non-filtered dataset, whereas 9.2 million points represent the ground points are depicted in Fig. 10B. It presents the scarps that were forming in the rough terrain. However, for landslide interpretation the 3D point cloud representation is less useful than the anaglyph images produced from the openness image.

4.5. ALS point density on landslide recognition

The thinned out datasets ranged from a point density of 1.69 to 27.20 points m^{-2} (Table 6). Fig. 11 shows a detail of the Bois Noir area, visualized as openness images. Three datasets are shown, the original, and thinned out data sets at levels 3 and 8. The visual assessments by experts started on the dataset with level 8 then followed by the other levels including the original dataset. The experts all agreed that the thinned dataset could be used to recognize the major geomorphological indicators of landslide activity. However, in order to differentiate the minor relief, recognize individual landforms and properly assess the landslide activity, point densities at levels 1–3 are required.

5. Discussion and conclusions

In this study, we evaluated the suitability of various types of ALS-derived DTMs for mapping landslides and for identifying morphological features of landslides. We used a quantitative measure for expressing the accuracy of the landslide DTMs based on ALS data and we investigated the usefulness of different visualization techniques on the interpretability of the landslide morphology. The vertical accuracy of the DTM varied between 0.28 and 0.36 m for the PTD filter. The accuracy depends on the types of geomorphological features. Our results are an improvement in accuracy compared to the previous studies that reported 0.57 m (Kraus and Pfeifer, 1998) and 0.46 m (Hodgson et al., 2003) vertical error over forested area. Reutebuch

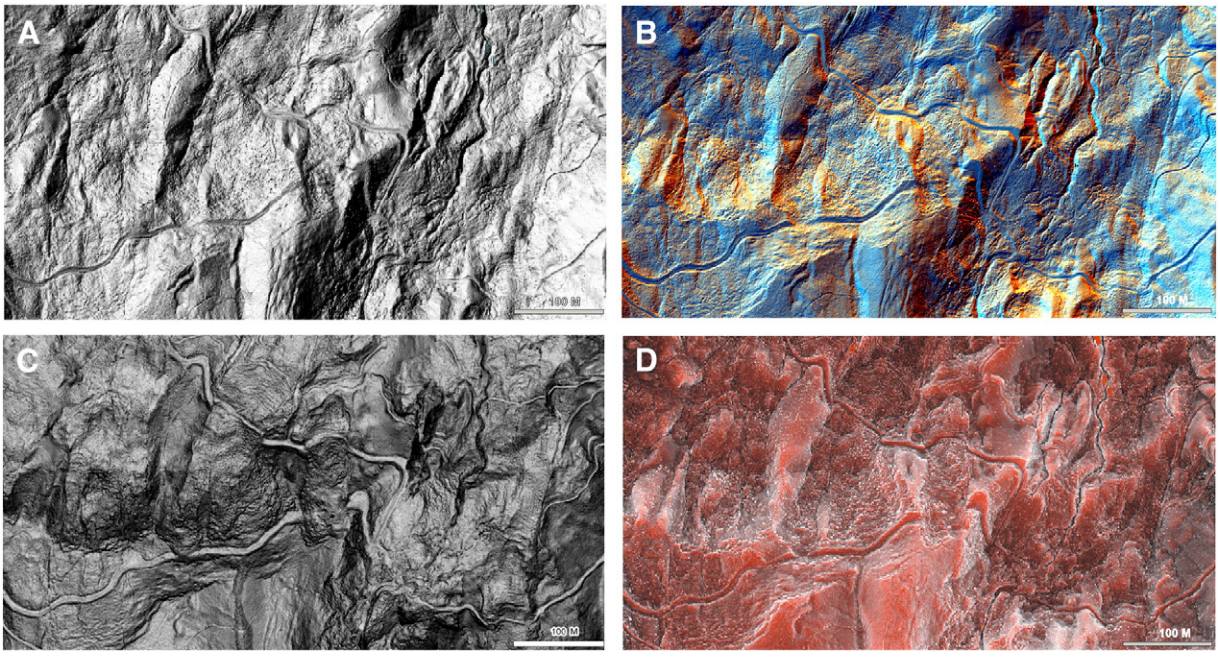

Fig. 8. Illustrations of the various visualization methods used for landslide interpretation. A) Shaded relief map. B) Colour composite map. C) Openness map. D) Red relief image map.

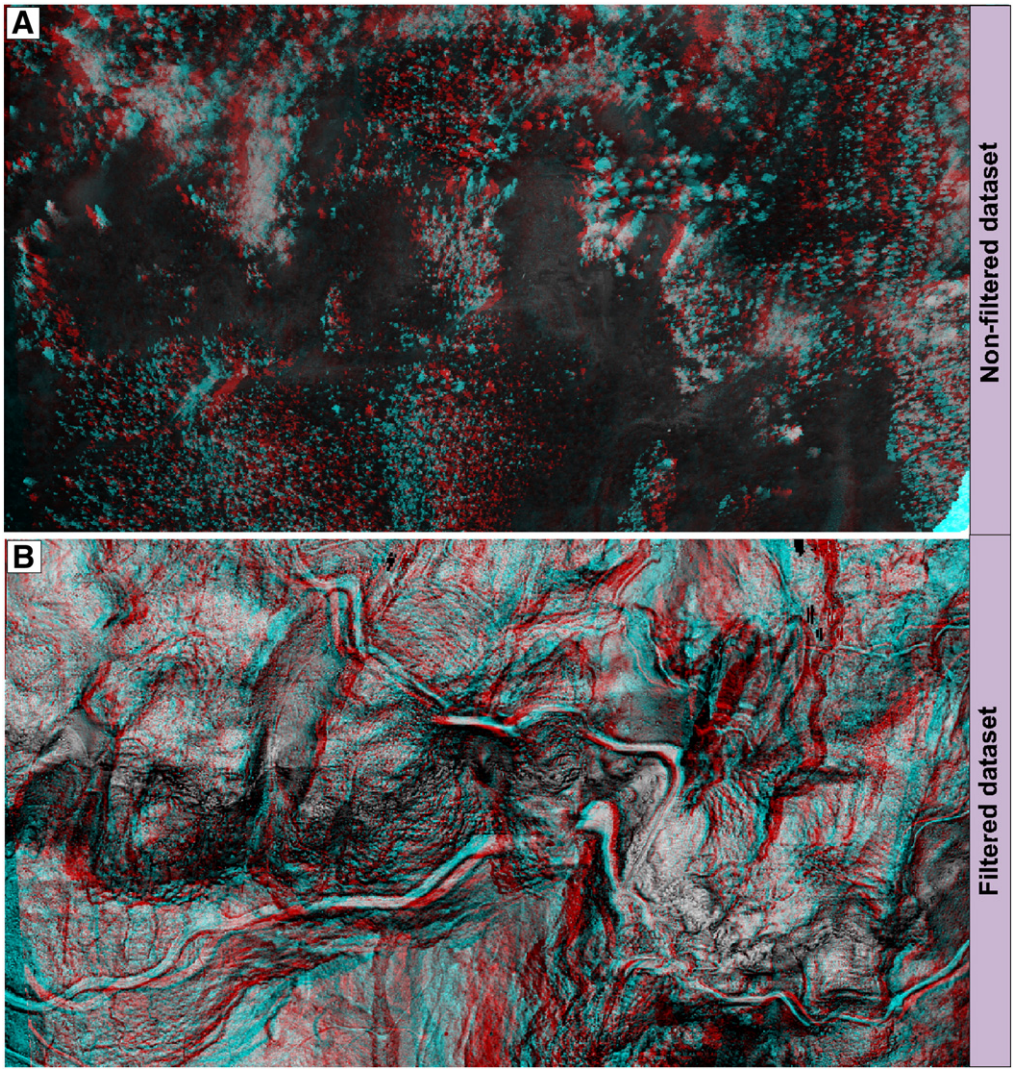

Fig. 9. Stereocopic models of non-filtered and filtered datasets. A) Anaglyph image showing dense vegetation covering the landslide area. B) Digital terrain model visualized as an openness image showing the morphology of forested landslides. Both images need to view with red-blue anaglyph glasses.

et al. (2003) and Wang and Glenn (2009) reported similar results for sloping forested terrain. The results from the different filter parameterizations of the HRI method were slightly less accurate, but still in the range between 0.30 and 0.40 m. The PTD filter yielded slightly lower RMSE than the landslide filter: about 0.28 and 0.33 m for morphological preservation and elimination of the trees, respectively. However, the landslide filter shows a better visualization for landslide recognition as depicted by expert image interpreters.

Pfeifer and Mandlburger (2009) state that the evaluation of an ALS-derived DTM under forest is difficult and expensive because it requires a higher precision of the ground control points than the ALS dataset and that reference points should be well distributed over the study area. In this work, however, we succeeded to carry out a thorough accuracy assessment. Under a dense canopy, the GPS signal was indeed too weak for a few cases to reach a high accuracy. We solved this problem by linking measurements acquired by a total station to GPS points outside the forest canopy.

The interpretation of slope movements from the ALS-derived DTM is based on the recognition or identification of elements associated with slope movements and the interpretation of their significance to slope instability. The ALS-derived DTM offers a significant improvement for landslide recognition and classification in forested terrain, as compared to optical images. Small morphological features, such as cracks, lateral ridges, pressure ridges and step wise morphology are clearly recognizable and gives the image interpreter unprecedented detail. Also the type of landslide is easily recognized from the detailed DTM. The trade-off between the four different filters is that trees were properly filtered out in the landslide and PTD filters, but rock blocks and the edges of incised channels are also filtered out. The HRI-default and forest filters maintained more of the trees, rock and channel edges. This trade-off is not shown in the accuracy assessment, but only showed up while interpreting the gridded DTM. This suggests that the HRI method with landslide filter parameterization would be a good method for DTM extraction of forested landslides, but that a separate filter should be applied when there is an interest in rock blocks and step edges.

The assessment of landslide activity using only the DTM was more difficult. This could be done much better if two ALS datasets were available from two different periods. Vegetation characteristics are important indicators of activity and these are normally obtained from aerial images. However, also with a high density ALS data the distribution pattern of irregular trees can be a good indicator for assessing landslide activity. The shape of the tree stem and the orientation of the tree may also be influenced by landslides. Back-

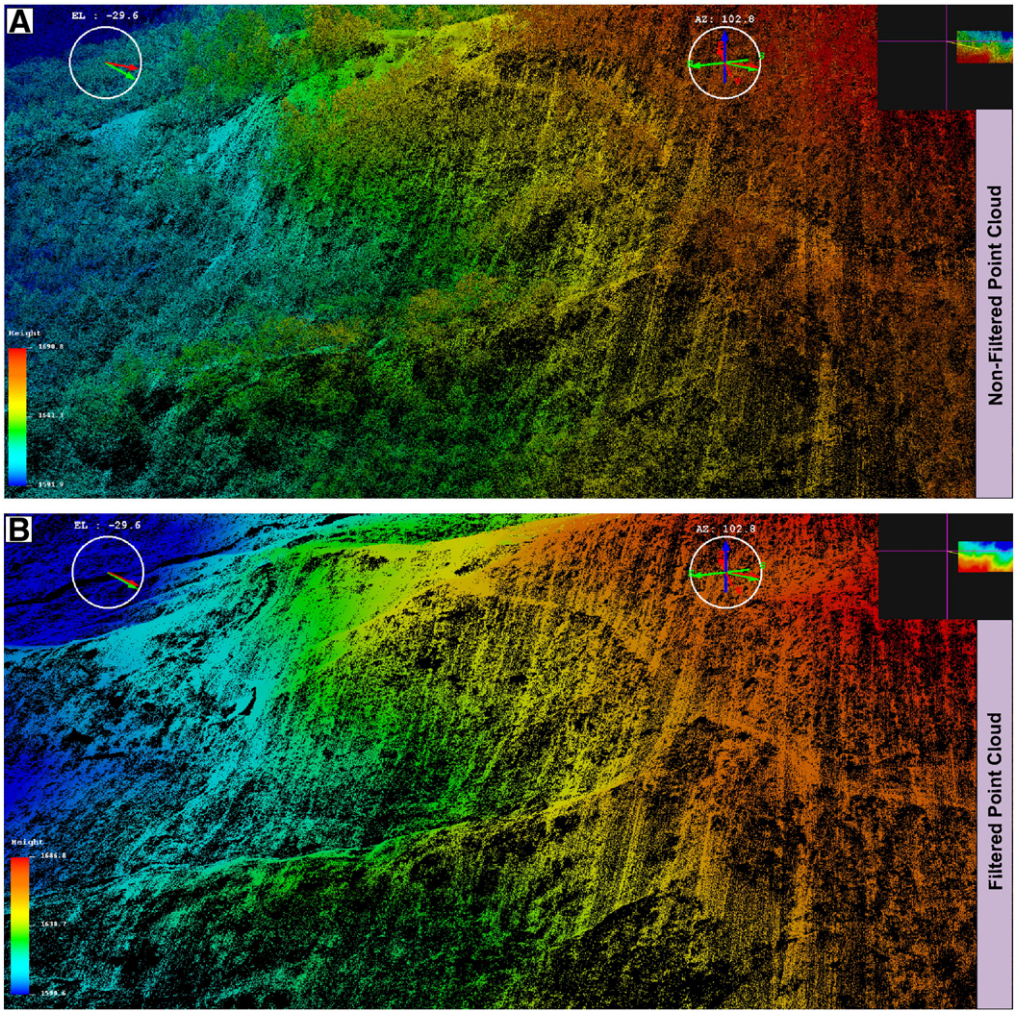

Fig. 10. 3D point cloud visualization of the Bois Noir landslide. A) 34.2 million points cloud representing the non-filtered dataset. B) Filtered ground points resulting in 9.2 million points cloud over the complex landslides.

tilting of trees indicate a rotational slide, whereas bended stems indicate slow motion of the top soil. These topics are currently being investigated.

While differences in the RMSE values differed little between the filters, the method of visualization had a large effect on the interpretability of the landslide. A stereoscopic model was used to visualize the landslides. The 3D view of the landscape gives a much stronger impression of the landscape dynamics than any of the monoscopic images. The interpretability of the 3D point cloud visualization was also less attractive than the stereo image due to the varying point densities across the area. For vegetation assessment the raw point cloud would be superior as at such a high point density the shape of the tree is clearly recognizable. The openness image showed most of the details in the area. It has a more natural view than the composite image and has the added advantage that the openness can be combined in a stereoscopic view as it is monochromatic. Shaded relief images proved less attractive due to the dependence on solar angle and the loss of detail in the end result.

The required point density for landslide interpretation depends on the purpose of the study. Gross morphological features of landslides are easily distinguished at a point density of 1.69 points m^{-2}. Detailed analysis of morphological features requires a point density more than 5.69 points m^{-2}. However for vegetation analysis, a very high density ALS data are preferable to enable detailed characterization of the shape of tree stems and branches (Bucksch and Lindenbergh, 2008).

This paper has shown the quality of an ALS-derived DTM for landslides mapping under a dense forest canopy. The generation of a detailed landslide inventory in forested terrain is considered important for landslide hazard assessment. This method should also be suitable in tropical areas where the re-vegetation of landslides proceeds rapidly. Furthermore, the vegetation characteristics, particularly on irregular trees extracted from high density ALS data could be used to assess landslide activity beneath a densely vegetated area.

Table 6
Thinning dataset with different horizontal distances and average point densities. The original dataset includes 12.6 million points with an average point density of 53 points m^{-2}.

Thinning Level	Horizontal distance (m)	Average point density (points m^{-2})	No. of points ($\times 10^6$)
1	0.25	27.20	6.50
2	1	12.37	2.96
3	3	5.69	1.36
4	5	3.80	0.91
5	7	2.84	0.69
6	9	2.32	0.55
7	11	2.00	0.46
8	13	1.69	0.40

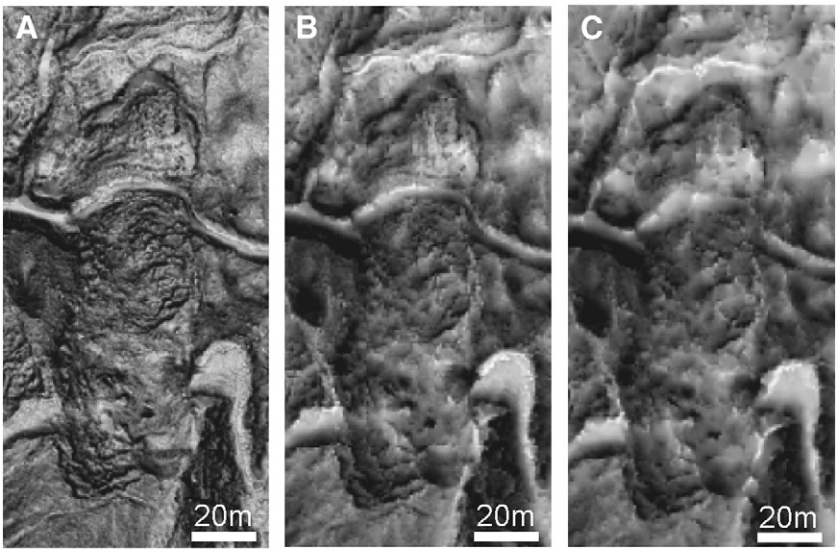

Fig. 11. Three examples of an openness map made from different point densities. A) Original dataset. B) Thinned level 3. C) Thinned level 8 (See also Table 6 for explanation of thinning levels).

Follow-up work is planned for landslides occurring in a forested tropical area with a case study in Malaysia.

Acknowledgements

The authors are grateful to the Malaysian Government for financing the first author's fellowship (SLAI-KPT/UTM) at the ITC-University of Twente, Netherlands and Faculty of Geosciences of Utrecht University, Netherlands. The ALS data acquisition has been provided through the funding from the French Project ANR Risk-Nat SISCA 'Système Intégré de Surveilllance de Glissements de Terrain Argileux' (2009–2021), from the Restauration des Terrains de Montagne (RTM, Division of Barcelonnette), and UNU-ITC School on Geoinformation for Disaster Risk Management. Thanks to Takahiro Hiramatsu (Asia Air Survey Co., Ltd.) for helping us in generating a red relief image map of the study area. Special thanks to Michiel Damen and Robert Voskuil who take part in landslide interpretation assessment.

References

Axelsson, P., 2000. DEM generation from laser scanner data using adaptive TIN models. International Archives of Photogrammetry and Remote Sensing 35, 110–117.

Brardinoni, F., Slaymaker, O., Hassan, M.A., 2003. Landslide inventory in a rugged forested watershed: a comparison between air-photo and field survey data. Geomorphology 54, 179–196.

Bucksch, A., Lindenbergh, R., 2008. CAMPINO — a skeletonization method for point cloud processing. ISPRS Journal of Photogrammetry and Remote Sensing 63, 115–127.

Chiba, T., Kaneta, S.I., Suzuki, Y., 2008. Red relief image map: new visualization method for three dimensional data. The International Archives of the Photogrammetry, Remote Sensing and Spatial Information Sciences vol. XXXVII, Part B2. Beijing, pp. 1071–1076.

Flageollet, J.-C., Maquaire, O., Martin, B., Weber, D., 1999. Landslides and climatic conditions in the Barcelonnette and Vars basins (Southern French Alps, France). Geomorphology 30, 65–78.

Glenn, N.F., Streutker, D.R., Chadwick, J., Glenn, D.J., Thackray, G.D., Dorsch, S.J., 2006. Analysis of LiDAR-derived topographic information for characterizing and differentiating landslide morphology and activity. Geomorphology 73, 131–148.

Hippolyte, J.C., Dumont, T., 2002. Identification of quaternary thrusts, folds and faults in a low seismicity area: examples in the Southern Alps (France). Terra Nova 12, 156–162.

Hodgson, M.E., Bresnahan, P., 2004. Accuracy of airborne lidar-derived elevation: emperical assessment and error budget. Photogrammetric Engineering and Remote Sensing 70, 331–339.

Hodgson, M.E., Jensen, J.R., Schmidt, L., Schill, S., Davis, B., 2003. An evaluation of LiDAR- and IFSAR-derived digital elevation models in leaf on conditions with USGS level 1 and level 2 DEMs. Remote Sensing of Environment 84, 295–308.

Hollaus, M., Wagner, W., Eberhofer, C., Karel, W., 2006. Accuracy of large-scale canopy heights derived from LiDAR data under operational constraints in a complex alpine environment. ISPRS Journal of Photogrammetry and Remote Sensing 60, 323–338.

Horn, B.K.P., 1981. Hill shading and the reflectance map. Proceedings of the IEEE 69 (1), 14–47.

Huising, E.J., Gomes Pereira, L.M., 1998. Errors and accuracy estimates of laser data acquired by various laser scanning systems for topographic applications. ISPRS Journal of Photogrammetry and Remote Sensing 53, 245–261.

James, L.A., Watson, D.G., Hansen, W.F., 2007. Using LiDAR data to map gullies and headwater streams under forest canopy: South Carolina, USA. Catena 71, 132–144.

Kasai, M., Ikeda, M., Asahina, T., Fujisawa, K., 2009. LiDAR-derived DEM evaluation of deep-seated landslides in a steep and rocky region of Japan. Geomorphology 113, 57–69.

Kraus, K., 2007. Photogrammetry, 2nd ed. Walter de Gruyter, Berlin.

Kraus, K., Pfeifer, N., 1998. Determination of terrain models in wooded areas with airborne laser scanner data. ISPRS Journal of Photogrammetry and Remote Sensing 53, 193–203.

Lopez Saez, J., Corona, C., Stoffel, M., Astrade, L., Berger, F., Malet, J.-P., submitted for publication. Dendrogeomorphic reconstruction of past landslide reactivation with seasonal precision: Bois Noir landslide, southern French Alps. Landslides.

Maquaire, O., Malet, J.-P., Remaitre, A., Locat, J., Klotz, S., Guillon, J., 2003. Instability conditions of marly hillslopes: towards landsliding or gullying? The case of the Barcelonnette Basin, South East France. Engineering Geology 70, 109–130.

McKean, J., Roering, J., 2004. Objective landslide detection and surface morphology mapping using high-resolution airborne laser altimetry. Geomorphology 57, 331–351.

Nichol, J.E., Shaker, A., Wong, M.S., 2006. Application of high-resolution stereo satellite images to detailed landslide hazard assessment. Geomorphology 76, 68–75.

Pfeifer, N., Mandlburger, G., 2009. LiDAR data filtering and DTM generation. In: Shan, J., Toth, C.K. (Eds.), Topographic Laser Ranging and Scanning: Principles and Processing. CRC/Taylor & Francis, pp. 307–333.

Pfeifer, N., Stadler, P., Briese, C., 2001. Derivation of digital terrain models in the SCOP++ environment. OEEPE Workshop on Airborne Laserscanning and Interferometric SAR for Detailed Digital Elevation Models, Stockholm, Sweden.

Pirotti, F., Tarolli, P., 2010. Suitability of LiDAR point density and derived landform curvature maps for channel network extraction. Hydrological Processes 24, 1187–1197.

Prokesova, R., Kardos, M., Medvedova, A., 2010. Landslide dynamics from high-resolution aerial photographys: a case study from the Western Carpathians, Slovakia. Geomorphology 115, 90–101.

Reutebuch, S.E., McGaughey, R.J., Anderson, H.E., Carson, W.W., 2003. Accuracy of a high-resolution LiDAR terrain model under a conifer forest canopy. Canadian Journal of Remote Sensing 29, 527–535.

Rott, H., 2009. Advances in interferometric synthetic aperture radar (InSAR) in earth system science. Progress in Physical Geography 33, 769–791.

Schulz, W.H., 2007. Landslide susceptibility revealed by LIDAR imagery and historical records, Seattle, Washington. Engineering Geology 89, 67–87.

SCOP++, 2008. The SCOP++ Software Manual. IPF, TU Vienna and INPHO Gmbh, Germany.

Sekiguchi, T., Sato, H.P., 2004. Mapping of micro topography using airborne laser scanning. Landslides 3, 195–202.

Sithole, G., Vosselman, G., 2004. Experimental comparison of filter algorithms for bare-earth extraction from airborne laser scanning points clouds. ISPRS Journal of Photogrammetry and Remote Sensing 59, 85–101.

Smith, M.J., Clark, C.D., 2005. Methods for the visualization of digital elevation models for landform mapping. Earth Surface Processess and Landforms 30, 885–900.
Szekely, B., Zamolyi, A., Drahanits, E., Briese, C., 2009. Geomorphic expression of neotectonic activity in a low relief area in an airborne laser scanning DTM: a case study of the Little Hungarian Plain (Pannonian Basin). Tectonophysics 474, 353–366.
Thiery, Y., Malet, J.-P., Maquaire, O., 2004. Observation on the activity of the Bois Noir landslide. Internal Report, EC-FP5 Alarm Project, Brussels. 10 pp.
Thiery, Y., Malet, J.-P., Sterlacchini, S., Puissant, A., Maquaire, 2007. Landslide susceptibility assessment by bivariate methods at large scales: application to a complex mountainous environment. Geomorphology 92, 38–59.
Vallet, J., Skaloud, J., 2004. Development and experiences with a fully digital handheld mapping system operated from a helicopter. The International Archives of Photogrammetry, Remote Sensing and Spatial Information Sciences vol. XXXV, Part B5. Istanbul, pp. 791–797.
Van Den Eeckhaut, M., Poesen, J., Verstraeten, G., Vanacker, V., Moeyersons, J., Nyssen, J., Van Beek, L.P.H., 2005. The effectiveness of hillshade maps and expert knowledge in mapping old deep-seated landslides. Geomorphology 67, 351–363.
Van Den Eeckhaut, M., Poesen, J., Verstraeten, G., Vanacker, V., Nyssen, J., Moeyersons, J., Van Beek, L.P.H., Vandekerckhove, L., 2007. Use of LIDAR-derived images for mapping old landslides under forest. Earth Surface Processes and Landforms 32, 754–769.
Van Westen, C.J., Lulie Getahun, F., 2003. Analyzing the evolution of the Tessina landslide using aerial photographs and digital elevation models. Geomorphology 54, 77–89.
Van Westen, C.J., Castellanos, E., Kuriakose, S.L., 2008. Spatial data for landslide susceptibility, hazard, and vulnerability assessment: an overview. Engineering Geology 102, 112–131.
Vosselman, G., Klein, R., 2010. Visualisation and structuring of point clouds. In: Vosselman, G., Maas, H.G. (Eds.), Airborne and Terrestrial Laser Scanning. Whittles Publishing. ISBN: 978-1904445-87-6, pp. 43–79.
Wang, C., Glenn, N.F., 2009. Integrating lidar intensity and elevation data for terrain characterization in a forested area. IEEE Geosciences and Remote Sensing Letters 6, 463–466.
Yokoyama, R., Shirasawa, M., Pike, R.J., 2002. Visualizing topography by openness: a new application of image processing digital elevation models. Photogrammetric Engineering and Remote Sensing 68, 257–265.